Title: Magnetic hardening induced in RCo5 (R = Y, Gd, Sm) by short HEBM

Author: Paweł Łopadczak, Anna Bajorek, Krystian Prusik, Maciej Zubko, Grażyna Chełkowska

Citation style: Łopadczak Paweł, Bajorek Anna, Prusik Krystian, Zubko Maciej, Chełkowska Grażyna. (2018). Magnetic hardening induced in RCo5 (R = Y, Gd, Sm) by short HEBM. "Acta Physica Polonica. A" (Vol. 133, no. 3 (2018), s. 688-690), doi 10.12693/APhysPolA.133.688

Proceedings of the European Conference Physics of Magnetism, Poznań 2017

Magnetic Hardening Induced in RCo_5 (R = Y, Gd, Sm) by Short HEBM

P. Łopadczak[a,b,*], A. Bajorek[a,b], K. Prusik[b,c], M. Zubko[b,c] and G. Chełkowska[a,b]

[a]A. Chełkowski Institute of Physics, University of Silesia in Katowice, Poland

[b]ŚMCEBI, University of Silesia in Katowice, Chorzów, Poland

[c]Institute of Materials Science, University of Silesia in Katowice, Chorzów, Poland

The paper is focused on the magnetic and structural properties of RCo_5 (R = Y, Gd, Sm) intermetallics fabricated by high energy ball - milling (HEBM). The investigated samples were first produced by arc-melting as bulk materials and then were milled for 1h in dimethylformamide with balls to powder ratio 10:1. The influence of the HEBM parameters on the microstructure was investigated by a variety of complementary measurement methods. The Rietveld refinement was performed to estimate the dependence of crystallite size and microstrain on type of sample. The hysteresis loops were recorded by SQUID magnetometer at 2 K and 300 K and at magnetic field up to $\mu_0 H = 7$ T. The impact of short HEBM process is visible as the enhancement of coercivity and simultaneous reduction of the saturation magnetization.

DOI: 10.12693/APhysPolA.133.688

PACS/topics: 81.07.–b, 81.07.Bc, 75.50.Ww, 75.60.–d, 75.75.Cd

1. Introduction

Recently, magnetically hard nanoparticles produced by ball milling have attracted great interest due to their various applications [1]. There exist several types of methods used for preparation of magnetically hard nanoparticles of intermetallic compounds including those via sputtering [2] and ball milling [3]. Among all the known materials, R–T based alloys have high magnetocrystalline anisotropy and therefore they are very desirable for potential applications. Recent studies reported a considerable progress in the synthesis of R–T [4] and Nd–Fe–B [4, 5] nanopowders via surfactant-assisted high energy ball milling (HEBM) as well as in the particle size selection of as-milled powders. However, the room temperature coercivity of synthesized nanoparticles having a diameter below 30 nm did not exceed 3 kOe. Due to the nature of HEBM a cold welding processes usually takes place, which lead to an increase in the average particle size. Therefore, the best approach for the preparation of magnetic nanopowders is to use an appropriate surfactant and organic carrier liquid, which enables to obtain nanoscale particles [4].

In this study, we have investigated the impact of HEBM on morphology and magnetic properties of selected RCo_5 (R = Y, Sm, Gd) alloys.

2. Experimental

YCo_5, $SmCo_5$ and $GdCo_5$ alloys were prepared by arc melting using pure metals. The ingots were annealed for 24h at 1100 °C. The pulverizing techniques included crushing the homogenized alloys, preliminary grinding in the agate mortar, and further HEBM with a Retsch Mixer Mill 400 were applied. The wet HEBM was carried out by using dimethylformamide (DMF) in 2ml Eppendorf vials and 2mm balls of ZnO_2 as the milling media with the balls to powder ratio of about 10:1 [8]. The short HEBM for 1h was applied into three studied samples. The crystal structure and morphology of selected samples were examined by using X-ray diffraction (XRD) with Empyrean PANalytical diffractometer with the Cu as X-ray source. The scanning electron microscopy (SEM) was performed with a JEOL JSM-7100F FEG (field emmission gun) high resolution scanning electron microscope (HR-SEM) operated at 15 kV in SE (Secondary Electron) mode. The hysteresis loops were measured with the SQUID magnetometer (Quantum Design MPMS XL7) at 2K and 300K.

3. Results

Figure 1 shows the X-ray data for the bulk crystalline as well as for $t = 1$ h as-milled samples. All samples crystallize in the 1:5 hexagonal $CaCu_5$ type of crystal structure. X-ray data did not reveal the presence of R and T oxides during the short milling process. Table I represents results from Rietveld refinement method performed in MAUD software with the maximum refinement factors of about $R_{wp} = 4.2\%$ and $R_p = 4.3\%$. As it is shown, the value of the a lattice parameter for $GdCo_5$ and $SmCo_5$ decreases with the pulverization degree whereas for YCo_5 sample its value increases. Simultaneously, the c lattice parameter exhibits a slight change for all samples. Thus, the volume of the unit cell for two samples (R = Sm, Gd) decreases and for R = Y increases which may suggest the slight contraction and expansion of the crystal lattice respectively. As one may notice the XRD peaks are broadened over milling points to the reduction in the crystallites size. The mean sizes of the nanocrystallites

*corresponding author; e-mail: pawel.lopadczak@smcebi.edu.pl

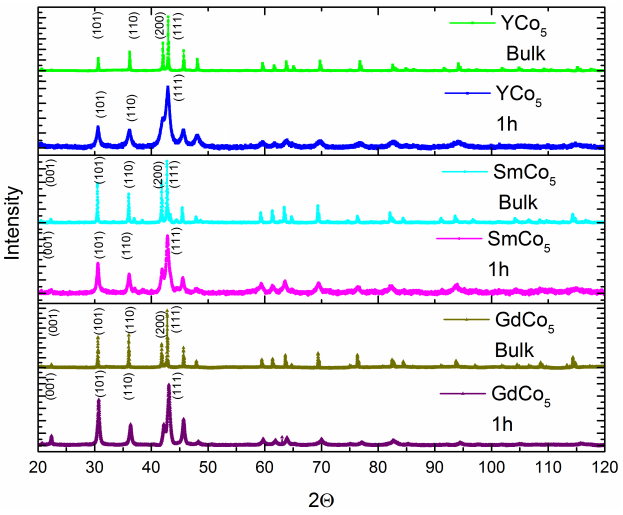

Fig. 1. The evolution of the XRD diffraction patterns upon milling for the crystalline and as 1h milled samples.

TABLE I

Crystal structure parameters for RCo_5 samples.

Sample	a [Å]	c [Å]	d [nm]	Strain r.m.s
bulk $GdCo_5$	4.968 $\pm 9.62_{.10^{-5}}$	3.957 $\pm 1.49_{.10^{-4}}$	263.91 ± 15.13	$4.84_{10^{-4}}$ $\pm 0.20_{.10^{-5}}$
1 h	4.944 $\pm 7.36_{.10^{-5}}$	3.971 $\pm 8.00_{.10^{-5}}$	28.81 ± 0.08	$1.18_{10^{-3}}$ $\pm 3.30_{.10^{-5}}$
bulk $SmCo_5$	4.977 $\pm 5.16_{.10^{-5}}$	3.981 $\pm 9.83_{.10^{-5}}$	526.60 ± 35.08	$4.45_{10^{-4}}$ $\pm 1.69_{.10^{-5}}$
1 h	4.974 $\pm 1.96_{.10^{-4}}$	3.987 $\pm 2.86_{.10^{-4}}$	21.91 ± 0.16	$8.14_{10^{-4}}$ $\pm 1.43_{.10^{-4}}$
bulk YCo_5	4.954 $\pm 4.83_{.10^{-5}}$	3.962 wyn7.67-5	259.83 ± 7.37	$1.20_{10^{-4}}$ $\pm 4.36_{.10^{-5}}$
1 h	4.970 $\pm 2.41_{.10^{-4}}$	3.975 $\pm 3.45_{.10^{-4}}$	15.27 ± 0.1	$2.09_{10^{-3}}$ $\pm 9.52_{.10^{-5}}$

were calculated according to Williamson-Hall method [6]. The observed drop in the d values during short milling process is driven by the deformation mechanism introduced into $CaCu_5$ lattice by HEBM. In this way the long range ordering degrades and is transformed into the short range one. So, the crystallites size for 1h ranges from 15.27 nm (R = Y) to 28.81 nm (R = Gd).

The hysteresis loops $M(H)$ for the crystalline as well as ball milled specimens measured up to 7 T at 300K and 2K are depicted in Fig. 2. The magnetic properties such as remanence M_R, saturation magnetization M_s, coercivity H_c and maximum energy product $BH_{\max}$ are evaluated from Fig. 2 and are displayed in Table II. For the bulk crystalline compound the magnetization at the maximum applied magnetic field almost reaches saturation. The values of the saturation magnetization estimated at 7 T and 2 K for the bulk samples suggest the rather ferrimagnetic arrangement between $4f$ and $3d$ sublattices.

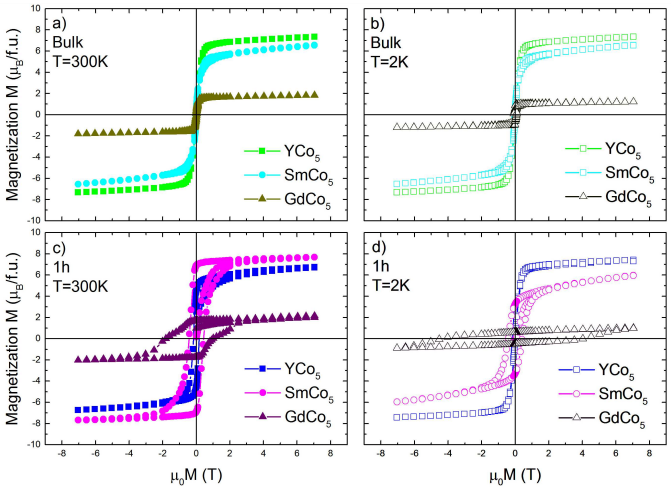

Fig. 2. Hysteresis loops for bulk as well as 1 h ball-milled samples.

TABLE II

Magnetic parameters for RCo_5 samples.

Sample	H_c [T]		M_R [μ_B/f.u.]		M_s [μ_B/f.u.]		$BH_{\max}$ [$\frac{kJ}{m^3}$]	
	300K	2K	300K	2K	300K	2K	300K	2K
bulk $GdCo_5$	0.025	0.085	0.37	0.85	1.83	1.21	0.33	5.19
1 h	0.990	4.050	1.68	0.61	2.14	1.00	8.02	32.13
bulk $SmCo_5$	0.014	0.058	1.45	1.44	6.54	6.11	0.09	2.91
1 h	0.438	0.239	6.92	7.62	7.69	8.35	129.7	32.03
bulk YCo_5	0.004	0.006	0.10	0.15	7.34	7.04	–	–
1 h	0.174	0.412	4.51	3.26	6.75	5.96	7.78	129.15

However, the obtained bulk materials show the value of M_s slightly lower than previously evidenced [13]. For the powdered samples the value of M_S generally increases. Moreover, as it was expected the values of H_c and M_R drasticly increase for all studied nanopowders. It may be attributed to a particles/grains size refinement and subsequent variation within magnetic interactions. The highest maximum energy product for the samples magnets is found to be $BH_{\max}$ = 129.7 kJ/m^3 for R = Sm. In the case of R = Gd despite the quite high coercivity its remanent magnetization is lower than for R = Sm and therefore the final $BH_{\max}$ value is also lower.

Furthermore, the short grinding induces a minor exchange bias (EB) effect, where hysteresis loops are shifted along H axis, as it was already evidenced in many types of nanomaterials but also even for some bulk compounds [2]. The value of the exchange bias field (H_{EB}) can be estimated as $H_{EB} = |H_{C+} + H_{C-}|/2$ and the average coercivity as $H_C = |H_{C+} - H_{C-}|/2$. For the studied $GdCo_5$ compound after 1h the hysteresis loop are shifted towards negative applied magnetic field, for the $SmCo_5$ powders towards positive applied magnetic field and for YCo_5 the shift is negligible. The maximum

value of H_{EB} is estimated for R = Gd at 300K and equals about H_{EB} = 0.16 T. Usually, in compound indicating the emergence of EB phenomenon, the hysteresis loop is often deformed. The induced EB for the granular alloys may be dependent on the particles microstructure, their surface roughness and sizes [10]. For milled powders the H_{EB} should increase with the reduction within particles size, but in the case of large surface-to-volume ratio EB effect may not occur.

Basing on the Stoner–Wohlfarth (S-W) model the remanence–to–saturation (M_R/M_S) ratio was estimated for various nanomaterials [11]. As it is well known the M_R/M_S dependence is dependent on the particles/crystallites size and shape as well as on the variation of anisotropy induced by an external magnetic field. For all powdered samples we can observe the increase of M_R/M_S ratio compared to the bulk parent compounds. The highest value of M_R/M_S is evidenced for R = Sm powder (M_R/M_S = 0.9) and the lowest for R = Y powder (M_R/M_S = 0.54). The values of remanence - to - saturation ratio obtained for powders is higher than 0.5, that is higher than predicted by S-W model. Usually, such order of magnitude of M_R/M_S is typical for hard nanocrystalline magnets indicating large exchange coupling between grains [12]. In our case this process also occurs, especially that the value of $BH_{\max}$ varies similary like M_R/M_S ratio.

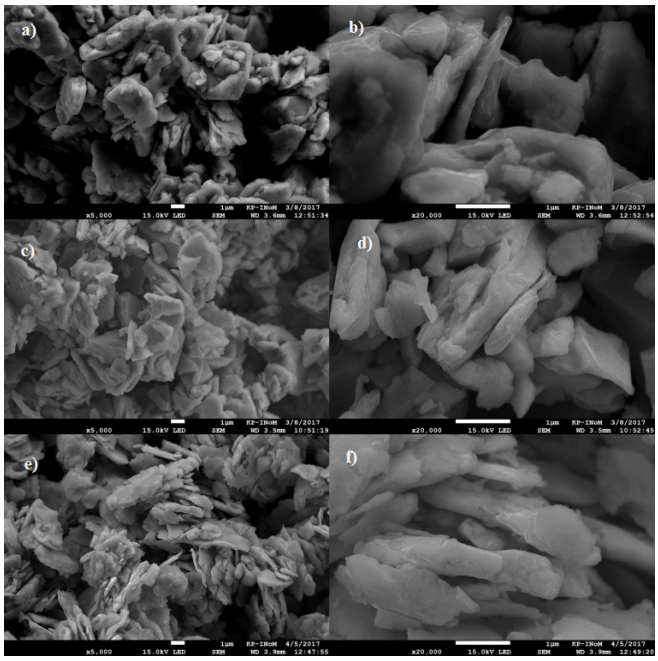

Fig. 3. The SEM images for the as-milled powders after 1 h for (a–b) YCo_5; (c–d) $SmCo_5$ and (e–f) $GdCo_5$.

The morphology of the as-milled powders was examined by SEM operated at 15 kV. The images were taken in the SE mode in the magnification range of 1000 to 20 000 times. The analysis of SEM images shows the presence of coarser powder which consists of with inhomogeneous particles having an average size from a few tens of microns to about a few microns. Among them there are visible single irregular flaked particles with a thickness ranging from 158 ± 48 nm for YCo_5 up to 247 ± 67 nm for $SmCo_5$. By analyzing the magnified images (see Fig. 3) one may easily notice a variety of microcracks on the particles surface, indicating that the short HEBM can be extended in order to obtain finer powders as it was previously evidenced for other R–T nanopowders [7, 8].

4. Conclusions

The results obtained for the bulk crystalline compounds and its as–milled powders exhibit the modification within crystal structure related to the reduction of crystallites size. The produced powder is non-homogeneous and the average particles size is around 200 nm. The short HEBM has a significant impact on magnetic properties. The change of the hysteresis loops suggest the presence of magnetic hardening induced by mechanical milling. The visible enhancement of coercivity, remenence and maximum energy product is beneficial due to potential applications. Summarizing, our approach indicates a significant potential for cost effective fabrication of RCo_5 nanomaterials via HEBM method having enhanced magnetic parameters in comparison to their bulk parent compounds. However, perhaps the applied synthesis requires further modification of various HEBM parameters in order to optimize the final structure, size, shape and magnetic behaviour of the as–milled powders.

References

[1] S. Sun, C.B. Murray, D. Weller, L. Folks, A. Moser, *Science* **287**, 1989 (2000).

[2] S. Stoyanov, V. Skumryev, Y. Zhang, Y. Huang, G. Hadjipanayis, J. Nogues, *J. Appl. Phys.* **93**, 7592 (2003).

[3] E.M. Kirkpatrick, S.A. Majetich, M.E. McHenry, *IEEE Trans. Magn.* **32**, 4502 (1996).

[4] V. M. Chakka, B. Altuncevahir, Z. Q. Jin, Y. Li, J. P. Liu, *J. Appl. Phys.* **99**, 08E912 (2006).

[5] H.G. Cha, Y.H. Kim, C.W. Kim, H.W. Kwon, Y.S. Kang, *J. Phys. Chem. C* **111**, 1219 (2006).

[6] P. Scherrer, *Gött. Nachr.* **2**, 98 (1918).

[7] L. Zheng, B. Cui, L. Zhao, W. Li, G.C. Hadjipanayis, *J. Alloys Compd.* **539**, 69 (2012).

[8] A. Bajorek, P. Skornia, K. Prusik, M. Wojtyniak, G. Chełkowska, *Materials Characterization* **101**, 58 (2015).

[9] P.D. Kulkarni, S.K. Dhar, A. Provino, P. Manfrinetti, A.K. Grover, *Phys. Rev. B* **82**, 144411 (2010).

[10] K.L. Liu, S.L. Yuan, H.N. Duan, X.F. Zheng, S.Y. Yin, *J. Appl. Phys.***107**, 023911 (2010).

[11] P. Saravanan, M. Premkumar, A.K. Singh, R. Gopalan1, V. Chandrasekaran, *J. Alloys Compd.* **408**, 645 (2009).

[12] N. Poudyal, B. Altuncevahir, V. Chakka, K. Chen, T.D. Black, J.P. Liu, Y. Ding, Z.L.Wang, *J. Phys. D: Appl. Phys.* **37**, L45 (2004).

[13] K.H.J. Buschow, *Rep. Prog. Phys.* **40**, 1179 (1977).